

Studies on Hydrogeochemistry and Human Health Risks of Groundwater in Hazaribag City, Jharkhand, India

NEERAJ KUMAR AND SHUBHA SRIVASTAVA*

Department of Chemistry, Vinoba Bhave University, Hazaribag, 825301, Jharkhand, India

E-mail: nkverma8539@gmail.com, shubhakbw@gmail.com

*Corresponding author

ABSTRACT

In the present paper, the groundwater quality of the selected places of Hazaribag City in Jharkhand, India, has been reported. In this connection results of the analyses of different physicochemical variables, including pH, electrical conductivity (EC), total dissolved solids (TDS), temperature, cations (Ca^{2+} , Mg^{2+} , Na^+ , K^+), anions (CO_3^{2-} , HCO_3^- , Cl^- , F^- , SO_4^{2-} , NO_3^-) and trace metals (Mn, Fe, Pb, Cr, Zn, Al, As) have been described. According to the Schoeller's diagram, the major cations, anions, and Heavy metals in the samples are in the order of $\text{Ca}^{2+} > \text{Na}^+ > \text{Mg}^{2+} > \text{K}^+$, $\text{HCO}_3^- > \text{Cl}^- > \text{SO}_4^{2-} > \text{NO}_3^-$ and $\text{Zn} > \text{Fe} > \text{Mn} > \text{Al} > \text{Cr} > \text{As} > \text{Pb}$, respectively. The Gibbs Plot indicates that the rock-water interaction mechanism is dominant, although the Piper plot demonstrates that groundwater samples are the mixed regions of $\text{Ca}^{2+} - \text{Mg}^{2+} - \text{Cl}^- - \text{SO}_4^{2-}$ and $\text{Ca}^{2+} - \text{Mg}^{2+} - \text{HCO}_3^-$ type reflecting the prevalence of anthropogenic influence. According to the Durov plot, 9.37% of groundwater samples exhibit association with dolomite or ion-exchange clay, 53.13% shows normal dissolution or mixing, and the rest 37.5% reverse ion-exchange of sodium and chloride type water. Groundwater in Hazaribag City is supersaturated with calcite, dolomite, and gypsum, while most of the samples are nearly at equilibrium with anhydrite. Conversely, all 32 groundwater samples are undersaturated with halite. The water quality index (WQI) shows that 9% of the samples of groundwater are good, 6% poor, 13% very poor, and the rest 72% are unfit for drinking. Positive correlations were observed among all water quality indices and heavy metals. The presence of heavy metals significantly contributed to non-carcinogenic health risks for both adults and children, following the order of $\text{Cr} > \text{As} > \text{Fe} > \text{Pb} > \text{Mn} > \text{Zn} > \text{Al}$.

Key words: Gibbs diagram, Piper plot, Physico-chemical variables, Saturation Index, Spatial distribution, Water quality

INTRODUCTION

Water is a fundamental need for life and its quality decides whether it is fit for drinking, bathing, irrigation and specific industry. Excessive use of groundwater and urban development has impacted the quality of groundwater. The quality of water is directly linked to human Health (Kumar et al. 2018). Many scientists conducted thorough investigations for hydrogeochemical analysis, water resources engineering, and water quality assessment (Todd 1980, Prince 1985, Karanth 1987). Information about the variations in the chemical composition of groundwater is provided through hydrogeochemical analysis. The quality of groundwater is solely determined by the interactions that occur between water and the different types of rocks and soil found along the pathway of groundwater saturation (Olayinka et al. 1999). Groundwater flows from recharge to discharge by a number of processes, including precipitation, ion exchange, mixing, redox

reaction, dissolution, and leaching. The presence of chemical components in groundwater is primarily due to interactions between the water and the surrounding rock or soil (Foster et al. 2000, Chidambaram et al. 2008). The sources of contaminated water might be either natural or man-made. This motivated the authors to assess the groundwater quality, hydrogeochemistry and its theoretical effects on human health in Hazaribag city, Jharkhand.

STUDY AREA

Locations

The Hazaribag city is located at latitude $23^{\circ}59'0''$ N and longitude $85^{\circ}21'0''$ E and is headquarters of North Chotanagpur division of Jharkhand state in India (Fig. 1). According to 2011 census report, Hazaribagh municipal area has a population of 142,489.

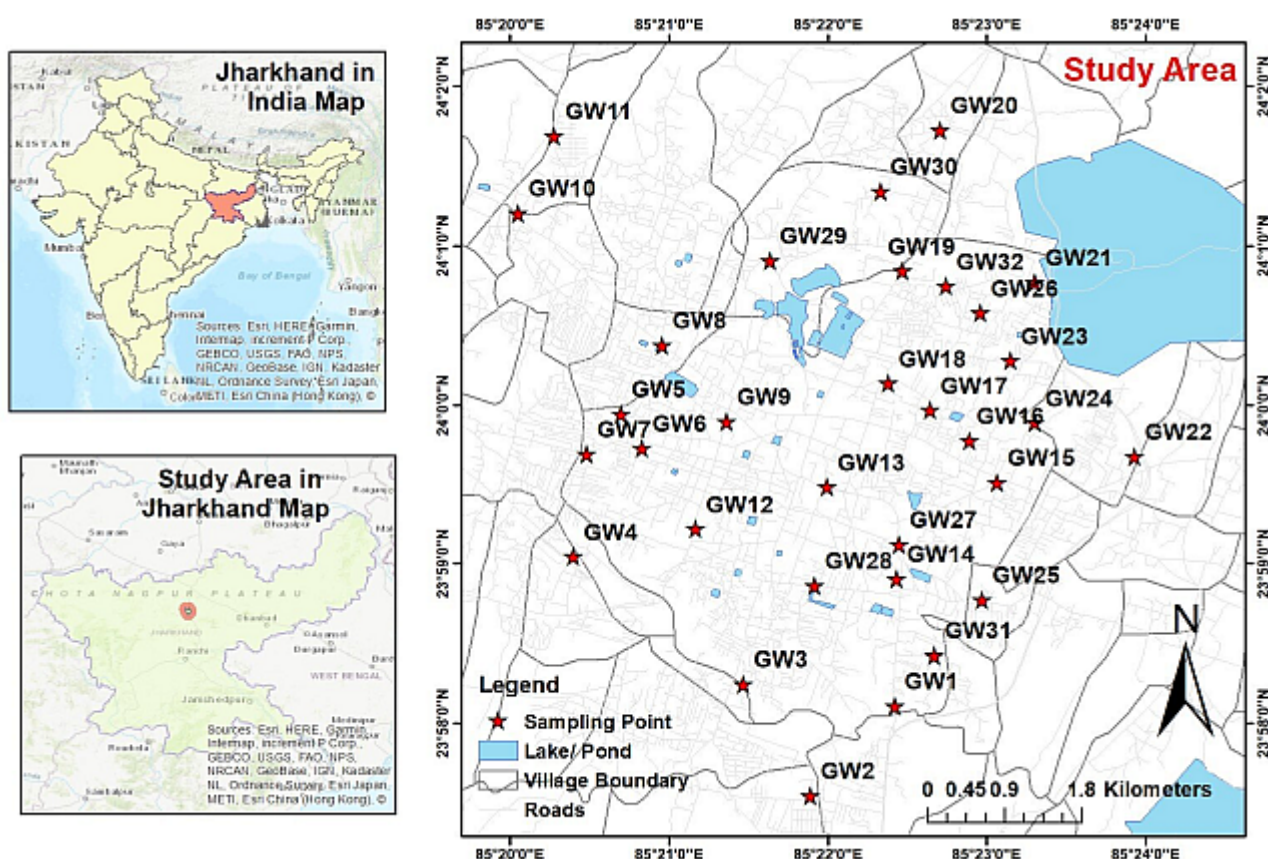


Figure 1. Map of the study area and sample locations

Geology

The geology of the study area is characterized by Chotanagpur granite gneiss, phyllite-mica-schist formations. Overlying these formations are lower Gondwana formations consisting of Sandstone, Shales, and Coal seams. Groundwater is predominantly found in weathered residuum under the water table and in deeper fractures under semi-confined conditions. Granite rocks exhibit a thick weathered mantle in areas with favorable topography and drainage.

Climate

The well-defined monsoon season in the Hazaribag typically lasts from the middle of June to the beginning of October. In summer, the temperature reaches a maximum of 46°C, while in winter it drops to a minimum of 4°C. The average annual rainfall is 1347 mm.

METHODOLOGY

Sampling and physico-chemical analysis

Thirty-two samples of groundwater were taken from the research region (Fig. 1) using hand pumps and tube wells (depth 120 to 180 feet). Standard procedures were used for sampling and analysis (Anonymous 2006). A portable water and soil analysis kit (Electronics India, model no. 162) was used to assess the temperature, electrical conductivity (EC), total dissolved solids (TDS), and pH at the designated sampling location. Other parameters such as cations (Na^+ , K^+ , Ca^{2+} , Mg^{2+}), and anions (Cl^- , F^- , CO_3^{2-} , HCO_3^- , SO_4^{2-} , NO_3^-) were analyzed at the Chemistry Laboratory of Vinoba Bhave University, Hazaribag by standards method (Ramesh and Anbu 1996). Trace metals (Mn, Fe, Pb, Zn, Cr, As and Al) were analyzed using an Inductively Coupled Atomic Absorption Spectrophotometer. The analytical findings were cross-referenced with the suggested benchmarks provided by WHO (Anonymous 2017) and BIS (Anonymous 2012).

Assessment of the water quality

In order to determine the quality of water in the study region, the following indices were used:

Water quality index (WQI)

The WQI was computed in MS Excel using the standard formula and results were compared with standard WQI range (Brown et al. 1972).

$$WQI = \sum_{i=1}^n W_i q_i \dots\dots\dots (i)$$

Where, W_i represents relative weight and q_i is the quality rating scale which can be calculated by using formula:

$$W_i = \frac{w_i}{\sum_{i=1}^n w_i} \dots\dots\dots (ii)$$

$$q_i = \frac{C_i}{S_i} \times 100 \dots\dots\dots (iii)$$

Where, w_i is weight assigned, C_i represents the individual parameter concentration, calculated by subtracting the observed concentration from the ideal value in pure water (7 for pH and 0 for all parameters). S_i denotes the BIS standard limit value for each parameter.

Heavy metal pollution index (HMPI)

The calculation of the HMPI is one of the best methods by which to represent the whole water qualities of water contamination of heavy metals (Mohan et al. 1996, Tamasi and Cini 2004). There are typically two processes involved in determining HPI, (i) assigning unit weights (W_i) to each water quality measure, and (ii) the sub-index value (Q_i), and then computing HMPI using the following equation:

$$W_i = \frac{K}{S_i} \dots\dots\dots (iv)$$

$$Q_i = \sum_{i=1}^n \frac{M_i - I_i}{S_i - I_i} \times 100 \dots\dots\dots (v)$$

$$HPI = \frac{\sum_{i=1}^n W_i Q_i}{\sum_{i=1}^n W_i} \dots\dots\dots (vi)$$

Where, K is constant and is equal to one, S_i is the standard permissible limit value, I_i is the ideal value

and M_i is the monitored value of i^{th} parameters.

Heavy metal evaluation index (HMEI)

HMPI and HMEI provide comprehensive data on water quality with regards to heavy metals. The calculation of the HMEI value is based on the following equation:

$$HMEI = \sum_{i=1}^n \frac{HM_{conc.}}{HM_{MPC}} \dots\dots\dots (vii)$$

The parameter HM_{Conc} denotes the monitored concentration of a specific heavy metal, while HM_{MPC} represents the maximum allowable concentration for that particular heavy metal. In order to assess the contamination of groundwater by heavy metals, a threshold of 1.0 was established. If the HMEI value is less than 1.0, it is categorized as “Fit” for domestic use. Conversely, if the value exceeds 1.0, it is classified as “Unfit” (Singh et al. 2017).

Health risk assessment (HRA)

HRA of water samples were done theoretically by standard methods using equation (viii), (ix) and (x). Both adults and children were considered in this study. The standard parameters, authoritative values and input assumptions along with the reference doses (RfD) are used to assess the exposure to heavy metals through drinking groundwater (Anonymous 2010, 2012).

The calculation of Chronic Daily Intake (CDI) for heavy metals through the ingestion of groundwater was performed by applying the equation (viii) provided by the US Environmental Protection Agency (Means 1989, Wu et al. 2009).

$$CDI = \frac{C_{HM} \times DI \times ABS \times EF \times ED}{BW \times AT} \dots\dots\dots (viii)$$

The HQ (Hazard Quotient) is determined by dividing the average chronic daily intakes (CDI) of heavy metals consumed through groundwater by their respective oral reference doses (RfD). The RfD for each heavy metal can be obtained from the relevant sources (Mohammadi et al. 2019). The calculation of the HQ is as follows:

$$HQ = \frac{CDI}{RfD} \dots\dots\dots (ix)$$

The Health Index (HI) was computed to evaluate

the overall potential risk to human health resulting from the consumption of various trace metals found in groundwater. The computation procedure is carried out as follows:

$$HI = \sum_{i=1}^n HQ = HQ_{Mn} + HQ_{Fe} + HQ_{Pb} + HQ_{Zn} + HQ_{Cr} + HQ_{Al} + HQ_{As} \dots (x)$$

Hydrogeochemical analysis

The hydrogeochemical analysis was done by Aqua Chem 4.0 software using the direction of the use of the software. It was used to draw Piper trilinear plot, Durov plot, stabler diagram, and Schoeller diagram in order to evaluate the geochemical facies. The dominant hydrogeochemical facies and quality control mechanism is evaluated by Gibbs diagram using following equations (Gibbs 1970):

$$\text{Gibbs Ratio (for anion)} = \frac{Cl^{-}}{Cl^{-} + HCO_3^{-}} \dots (xi)$$

$$\text{Gibbs Ratio (for cation)} = \frac{Na^{+} + K^{+}}{Na^{+} + K^{+} + Ca^{2+}} \dots (xii)$$

The saturation index (SI) helps us to know the nature of water in contact with different kinds of rocks. When the SI is equal to zero, the minerals are in equilibrium with the water. A negative SI indicates that the minerals are unsaturated and likely to dissolve; while a positive SI indicates that the minerals are supersaturated, leading to deposition. The SI is defined as:

$$SI = \log \frac{IAP}{K} \dots (xiii)$$

The IAP (ion activity product) is a measure used to describe the dissolution of minerals in a chemical reaction. It is determined by the product of the ion activity coefficient (γ_i) and the ion concentration (M_i). The equilibrium constant (K) indicates the extent of mineral dissolution at a given temperature. In this context, the SI of significant minerals, including anhydrite, calcite, dolomite, fluorite, gypsum, and halite, was determined using the geochemical program PHREEQC (Parkhurst and Appelo 1999).

The spatial variation maps of important parameters (pH, EC, TDS, and TH), WQI, HMPI, HMEI, and EWQI were made using Inverse distance weighted (IDW) interpolation in ArcMap (version 10.8.2). The

degree of relation between various physicochemical parameters was interpreted through correlation analysis using the bivariate method and Pearson's correlation coefficient (Wu et al. 2014).

RESULT AND DISCUSSION

Physico-chemical analysis

Table 1 displays the analytical data of various physical and chemical parameters, as well as the concentrations of heavy metals found in the water samples. In order to assess the water quality, the standards established by the World Health Organization (Anonymous 2017) and the Bureau of Indian Standards (Anonymous 2012) were used as benchmarks. The subsequent discussion presents a summary of the obtained outcomes.

Physical parameters

The pH level of water is significantly influenced by the presence of calcium, magnesium, and sodium (Rao et al. 1982). The groundwater samples marked as standards except GW sample no. 5, 9, 12, 13, 19 and 20. The pH level influences the weathering pattern in the study area, regulating the presence of major ions in the water (Meybeck 1987). Figure 2a displays the spatial distribution map illustrating the pH levels of selected groundwater.

The EC of water is directly correlated with the concentration of ionized materials it contains and may also be associated with issues with increased hardness and some other mineral contaminants. 1000 $\mu\text{S}/\text{cm}$ is the recommended limit for EC for drinking water (Anonymous 2017). The electrical conductivity varies from 671.2 to 1482.4 $\mu\text{S}/\text{cm}$ with an average of 955 $\mu\text{S}/\text{cm}$. Figure 2b displays the spatial distribution map of groundwater EC.

Total dissolved solid (TDS) data is used to quantify the concentration of minerals dissolved in water. The main contributors to TDS in water include silica, sodium, potassium, calcium, magnesium, chlorides, bicarbonates, carbonates, sulfate, phosphate etc. TDS mostly affects the water supply system because of scale formation, a large amount of soap used, artery calcification, the formation for urinary concretions, renal or bladder disorders, and stomach problems (Gupta and Gupta 1987). According to WHO (Anonymous 2017), the desirable level of TDS is up to 600 mg/L, while the

Table 1. Physicochemical variables of groundwater of the study area and comparison with drinking water quality standards of WHO (Anonymous 2017) and BIS (Anonymous 2012).

Parameter	Unit	Minimum	Maximum	Mean	SD	WHO (2017)	BIS (2012)
Temp	°C	20.00	21.30	20.50	0.36	-	-
pH		7.18	8.92	8.02	0.45	6.5 – 8.5	6.5-8.5
EC	µS/cm	671.20	1482.40	955.00	214.10	1000	-
TDS	mg/L	441.20	951.10	624.20	136.90	600–1000	500
TH	mg/L	227.68	523.05	346.50	84.10	100–300	200
Ca ²⁺	mg/L	60.80	146.20	95.40	26.94	75	75
Mg ²⁺	mg/L	13.96	39.94	26.30	6.00	50	30
Na ⁺	mg/L	55.60	108.10	86.60	14.78	200	200
K ⁺	mg/L	2.89	26.30	10.53	4.77	12	<20
Cl ⁻	mg/L	65.40	161.50	109.90	22.80	200-300	250
HCO ₃ ⁻	mg/L	198.00	457.00	298.50	73.80	250	-
SO ₄ ²⁻	mg/L	42.80	131.20	82.40	23.47	250	200
F ⁻	mg/L	0.30	1.21	0.49	0.18	1	1.5
NO ₃ ⁻	mg/L	23.50	46.50	35.65	6.12	50	45
Al	mg/L	0.11	0.68	0.30	0.13	0.1	0.03-0.2
As	mg/L	0.01	0.02	0.01	0.00	0.01	0.01-0.05
Cr	mg/L	0.01	0.24	0.05	0.04	0.05	0.05
Fe	mg/L	0.33	1.93	0.85	0.37	0.3	0.3
Mn	mg/L	0.16	0.91	0.41	0.20	0.3	0.1 - 0.3
Pb	mg/L	0.00	0.09	0.02	0.03	0.01	0.01
Zn	mg/L	1.06	16.27	5.99	4.09	5	5-15

maximum acceptable limit is up to 1000 mg/L. Total dissolved solids (TDS) in the groundwater samples of the study area were found within acceptable limits. The spatial distribution map of TDS of groundwater is shown in Figure 2c.

Physically, hardness can be defined as the water resistance to soap lather. Total hardness (TH) is the combined concentration of Ca²⁺ and Mg²⁺, expressed as mg/L equivalents of CaCO₃, from a chemical perspective (Kaushik et al. 2002). Hardwater can cause scales in water heaters, and distribution pipes, and require extra soap when washing clothes. White encrustations on boilers and kitchen appliances are also a result of it (Karanth 1987). Hard water consumption can result in cardiovascular issues, urolithiasis, and various cancer diseases (Durvey et al. 1991, Agrawal and Jagetia 1997). The level of total hardness (TH) in the investigated region varies between 227.68 and 523.05 mg/l, averaging at 346.5 mg/l. According to the BIS (Anonymous 2012) recommendations, none of the groundwater samples obtained is considered safe for human consumption.

The spatial distribution of total hardness in groundwater is depicted in Figure 2d.

Major ions (Ca²⁺, Na⁺, Mg²⁺, K⁺, HCO₃⁻, Cl⁻, SO₄²⁻, NO₃⁻)

The graphical distribution of the major chemical ions has been plotted in the stabler diagram (Guettaf et al. 2014) (Fig. 3). The predominance of calcium and bicarbonate ions characterized the hydrogeochemistry of the water resources in the study region. The Schoeller diagram (Fig. 4a) predicts the order of major cations and anions as, Ca²⁺ > Na⁺ > Mg²⁺ > K⁺ and HCO₃⁻ > Cl⁻ > SO₄²⁻, > NO₃⁻, respectively. The origin of calcium ions is typically attributed to the dissolution of limestone, dolomites, gypsum, and anhydrite (Garrels 1976). In the present study area, where carbonate lithology is absent, the influence of carbonate weathering on water chemistry can be ruled out. Calcium is commonly derived from minerals like albite, hornblende, and plagioclase through the process of weathering. Furthermore, calcium ions can also be acquired through cation exchange mechanisms. The occurrence of

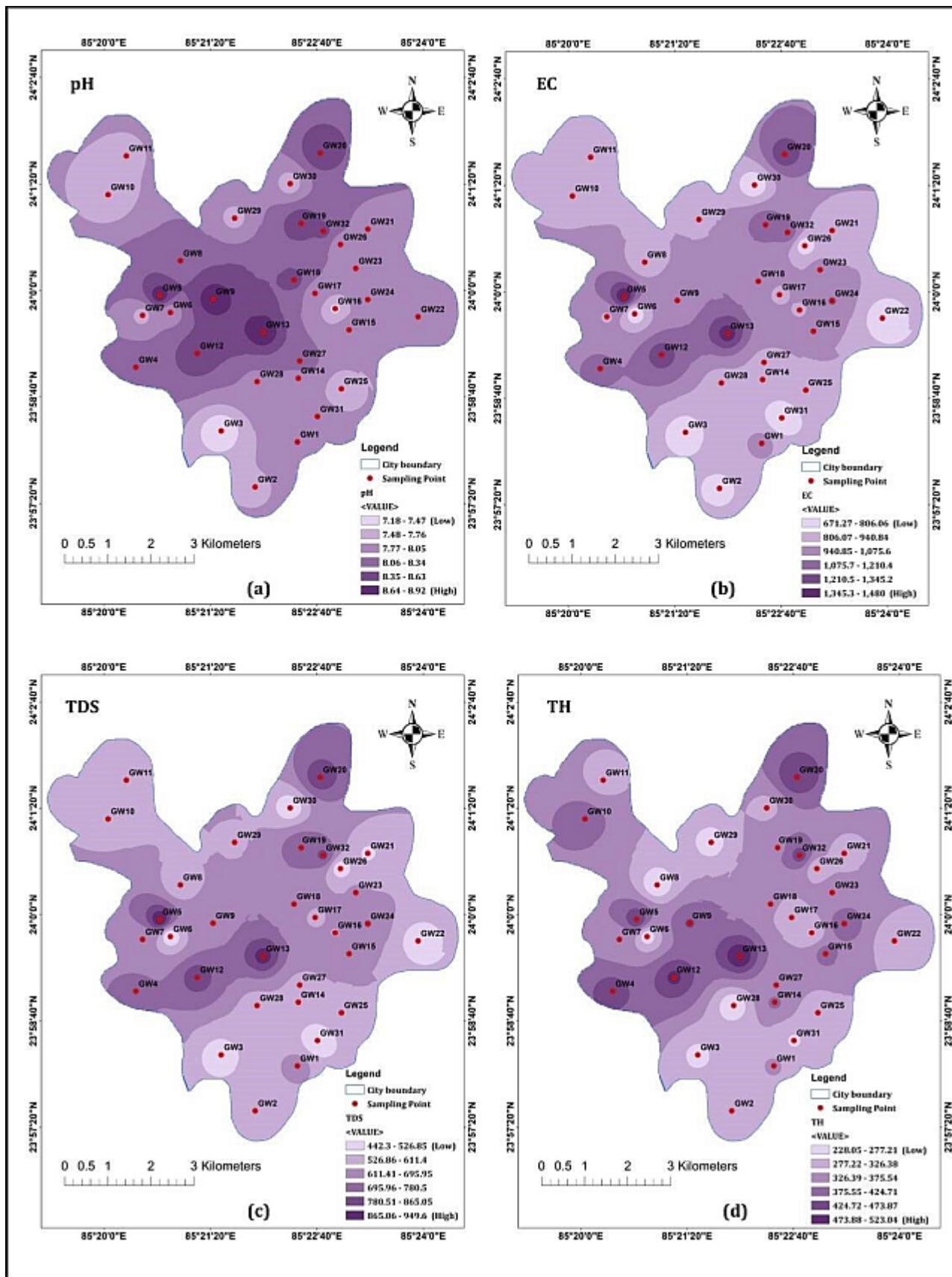


Figure 2. Spatial distribution map of (a) pH (b) EC (c) TDS (d) TH of groundwater of study region

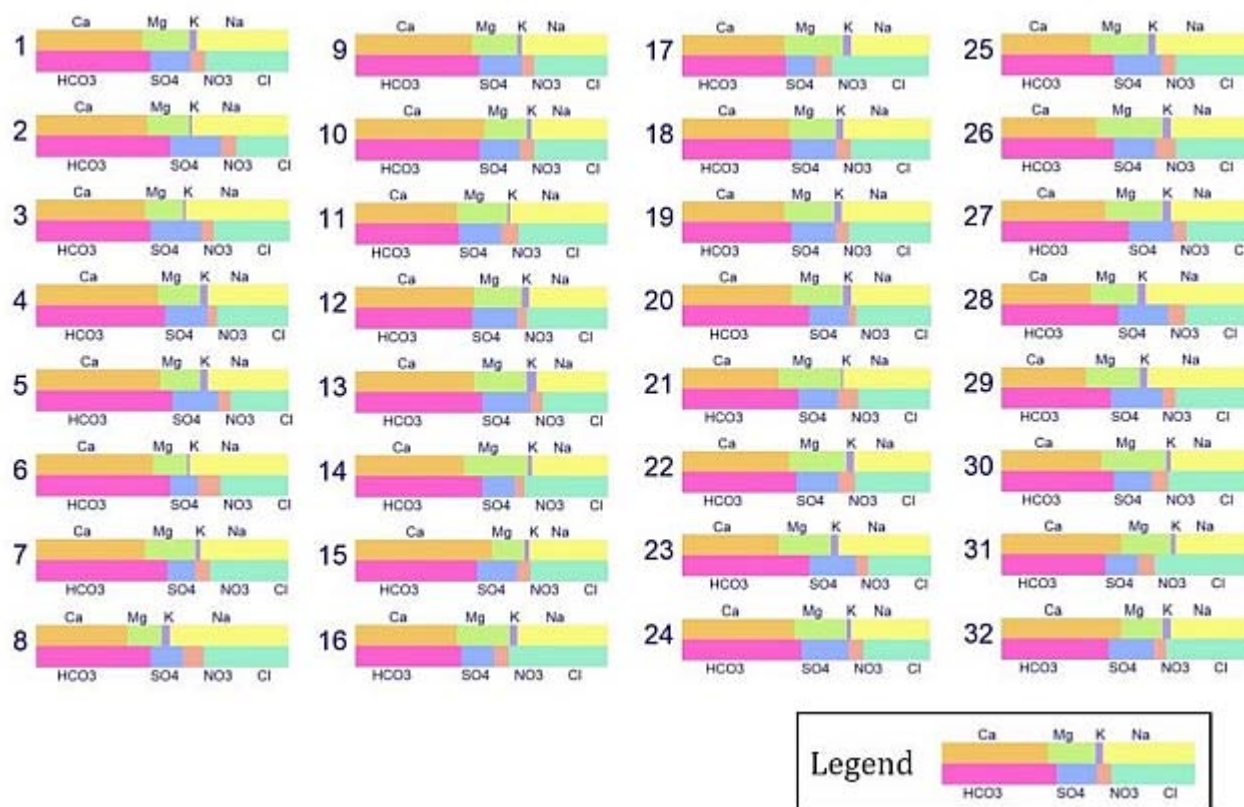


Figure 3. Stabler diagram illustrating major ionic dominance in the samples

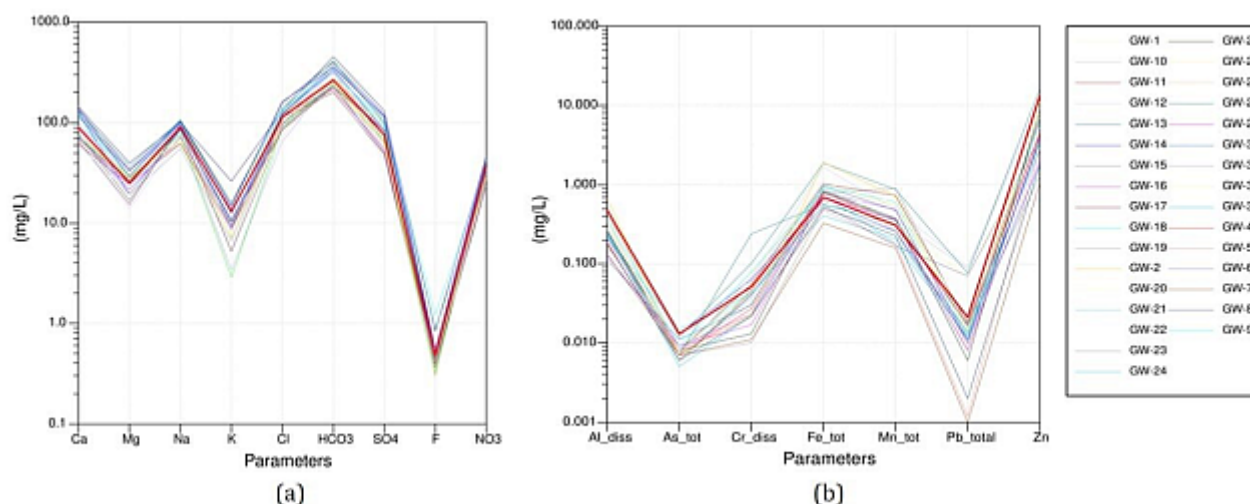


Figure 4. Schoeller diagram displaying the variation of (a) major ions and (b) Heavy metals (Scholler 1965)

magnesium ions in water can be attributed to either ion exchange processes or the weathering of minerals such as amphiboles, pyroxenes, and clay minerals. The prevalence of Na⁺ ions is most likely a result of the dissolution of alkali feldspar minerals within the aquifer. The weathering of K-feldspar releases potassium compounds into the water. All of the

groundwater samples of the study region are quite safe and ideal for drinking based on the potassium (except GW sample no. 13) and Magnesium limit set by Anonymous (2012, 2017).

The comparatively low concentration of Na⁺ and Cl⁻ indicates that there are no evaporite deposits or a saltwater intrusion process in the region (Hubbard

and Sheridan 1989). The concentration of HCO_3^- exceeded SO_4^{2-} , demonstrating that carbonic acid weathering predominates in the studied region and the bicarbonates may be derived from weathering of silicate rocks and minerals (silicate weathering). Sulfate ions originate from evaporate minerals like anhydrite and gypsum, as well as from the leaching of agricultural fertilizers.

The concentration of chloride may be due to residential waste, unsanitary circumstances, soil leaching, or inherent geochemical processes. It was found that the nitrate percentage was substantially below the standard limit for drinking water. So, there is no nitrate pollution in the samples.

Fluoride ion

The samples were also analyzed for F^- ion. The concentration varied from 0.3 to 1.21 mg/l, the average being 0.487 mg/l. Only GW 9 sample have higher value than acceptable limit. The higher concentration of F^- ion may be due to medical activity.

Heavy metals

The Schoeller diagram (Fig. 4b) was plotted for heavy metals and the order of dominance was found to be $\text{Zn} > \text{Fe} > \text{Mn} > \text{Al} > \text{Cr} > \text{As} > \text{Pb}$. In most of the groundwater samples Zn, Fe, Mn and Cr were found to above permissible limits. That may be due to the rusting of pipes of the tube well and borewell. Most of the samples higher value of Al than acceptable limit. This is due to the leaching of aluminum silicate. The presence of lead in the samples may be due to the anthropogenic activity.

Suitability of groundwater for drinking proposes

Water quality index (WQI)

The different classes of WQI for the consumption of groundwater are shown in Table 2. On comparison with standard water quality index, it has been found that 28% of the groundwater samples fall to good quality, 53% poor quality and 19% are unfit for consumption category. The primary factors contributing to the poor water quality may comprise issues related to sewerage and significant rock-water interaction (Krishna Kumar et al. 2013). The Spatial variation map of the WQI has been shown in Figure 5a. It is obvious from the map that water from a larger portion of the research area is unsafe for drinking.

Heavy Metal Pollution Index (HMPI)

The HMPI was utilized to evaluate the heavy metal levels in groundwater, offering valuable observations regarding the patterns and variations in groundwater quality (Singh et al. 2017). Table 2 summarizes the calculated HMPI values and their descriptions. The HMPI values ranged from 15.56 to 645.98, with a mean of 188.92. HMPI values exceeding 100 are considered critical pollution indices (Mohan et al. 1996). Classification of the samples revealed that 69% of the study region's sample locations had HMPI values above the critical pollution index. i.e., 100, and hence contaminated with heavy metals and are unsafe for drinking and the rest 31% of samples location have HMPI below 100 and are safe for human consumption. Spatial variation in HMPI indicates that a larger area of the study region is

Table 2. Classification of the groundwater quality of the study area based on calculated water quality index (WQI), heavy metal pollution index (HMPI), and heavy metal evaluation index (HMEI)

Index method	Category	Water quality status (WQS)	% Sample
WQI	<50	Excellent	-
	50-100	Good	28
	100-200	Poor	53
	200-300	Very Poor	-
	>300	Unfit for Consumption	19
HMPI	<100	Safe for Drinking	31
	>100	Contaminated with heavy metal	69
HMEI	<1.0	Fit	97
	>1.0	Unfit	3

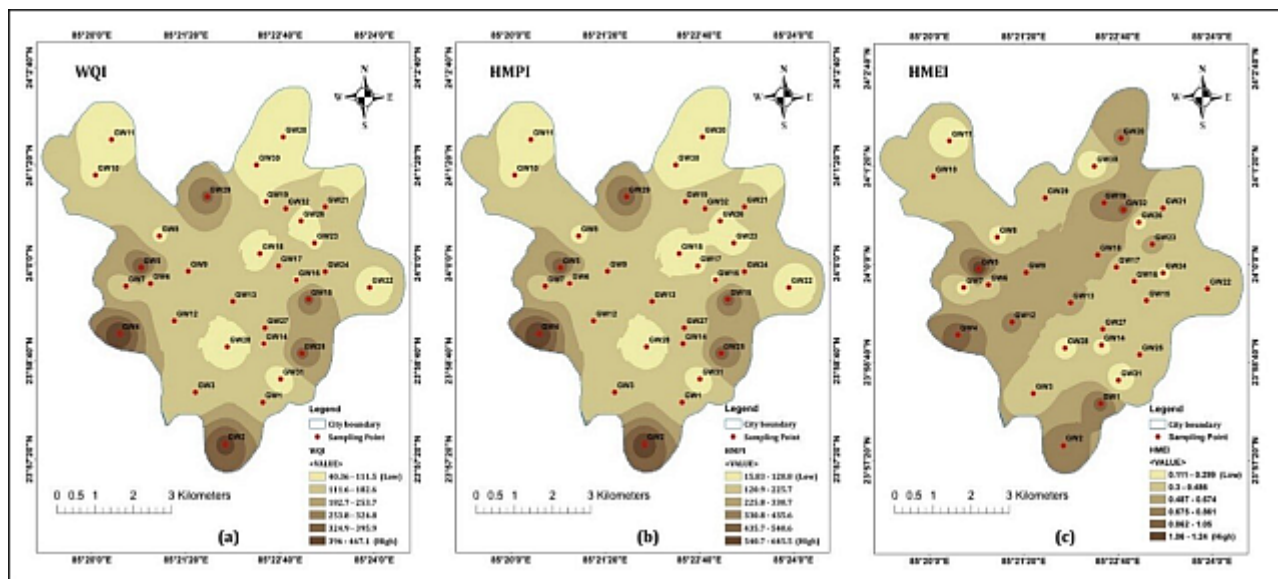


Figure 5. Spatial distribution map of (a) WQI (b) HMPI (c) HMEI of groundwater of study region

Table 3. Correlation coefficient matrix for water quality indices values and metal concentration

	HMEI	WQI	HMPI	Al	As	Cr	Fe	Mn	Pb	Zn
HMEI	1									
WQI	0.52**	1								
HMPI	0.49*	1.00**	1							
Al	0.47*	0.13	0.12	1						
As	0.32	0.20	0.12	0.15	1					
Cr	0.26	0.28	0.28	0.07	0.09	1				
Fe	0.70**	0.45*	0.44*	0.47	0.14	0.14	1			
Mn	0.45*	0.17	0.17	0.34	0.04	0.13	0.69	1		
Pb	0.47*	0.99**	1.00**	0.09	0.11	0.22	0.42	0.14	1	
Zn	0.99**	0.51**	0.48*	0.42	0.44	0.26	0.63	0.37	0.46	1

** means correlation is significant

contaminated with heavy metals (Fig. 5b). The HMPI values demonstrated significant positive correlations with the WQI and Pb, while displaying moderate correlations with Fe and Zn (Table 3).

Heavy metal evaluation index (HMEI)

The HMEI was calculated to assess groundwater quality regarding heavy metal contents, aiding in the identification and quantification of trends (Singh et al. 2017). Table 2 presents a summary of the computed HMEI values and their corresponding descriptions. The HMEI values varied between 0.107 and 1.236, with an average value of 0.479. With the exception of GW 5, all 32 groundwater samples obtained from Hazaribag City were classified as ‘Fit’.

Figure 5c illustrates the spatial distribution of HMEI. Correlations between HMEI values and other parameters were observed. Notably, HMEI showed significant positive correlations with WQI, Fe, and Zn, but only moderate correlations with HMPI, Al, Mn, and Pb (Table 3). Hence, the occurrence of significant quantities of heavy metals, particularly iron (Fe) and zinc (Zn), in the groundwater samples obtained from specific regions of the city, has led to their unsuitability for consumption as potable water.

Human health risk assessment

Human health risk assessment is a process that entails the examination of the adverse health effects experienced by individuals due to their exposure to

Table 4. Summary of the chronic health risk for adults and children of heavy metals in groundwater through oral ingestion

Health risks index	Heavy metal	Adults			Children		
		Min.	Max.	Mean	Min.	Max.	Mean
Hazard quotient (HQ)	Mn	1.66×10^{-3}	3.74×10^{-3}	2.36×10^{-3}	1.04×10^{-2}	2.50×10^{-2}	1.53×10^{-2}
	Fe	4.27×10^{-3}	1.31×10^{-2}	7.15×10^{-3}	2.74×10^{-2}	8.95×10^{-2}	4.75×10^{-2}
	Pb	4.88×10^{-3}	5.88×10^{-3}	5.13×10^{-3}	2.93×10^{-2}	3.63×10^{-2}	3.11×10^{-2}
	Zn	1.90×10^{-4}	2.16×10^{-3}	8.33×10^{-4}	1.31×10^{-3}	1.51×10^{-2}	5.77×10^{-3}
	Cr	5.81×10^{-2}	8.80×10^{-2}	6.29×10^{-2}	3.50×10^{-1}	5.59×10^{-1}	3.84×10^{-1}
	Al	2.14×10^{-5}	4.35×10^{-5}	2.85×10^{-5}	1.33×10^{-4}	2.88×10^{-4}	1.83×10^{-4}
	As	5.74×10^{-2}	5.87×10^{-2}	5.78×10^{-2}	3.45×10^{-1}	3.54×10^{-1}	3.48×10^{-1}
Hazard Index (HI)	-	1.26×10^{-1}	1.59×10^{-1}	1.36×10^{-1}	7.67×10^{-1}	9.91×10^{-1}	8.32×10^{-1}

hazardous substances, aiming to determine the potential risks involved. This study aimed to evaluate the potential non-carcinogenic health risks associated with drinking water, utilizing the guidelines recommended by the United States Environmental Protection Agency (Anonymous 2010). The average CDI values for Mn, Fe, Pb, Zn, Cr, Al, and As were 3.31×10^{-5} , 5.00×10^{-5} , 1.79×10^{-5} , 2.50×10^{-5} , 1.88×10^{-5} , 2.85×10^{-5} and $1.73 \times 10^{-5} \text{ mg kg}^{-1}\text{day}^{-1}$ for an adult and 2.14×10^{-4} , 3.31×10^{-4} , 1.08×10^{-4} , 1.73×10^{-4} , 1.15×10^{-4} , 1.82×10^{-4} and $1.04 \times 10^{-4} \text{ mg kg}^{-1}\text{day}^{-1}$ for the child, respectively.

Table 4 displays the statistical summary of HQ and HI values for adults and children. The average HQ values illustrate the extent of heavy metal impact on non-carcinogenic health risk for both

demographics. The order of heavy metals based on their contribution is as follows: $\text{Cr} > \text{As} > \text{Fe} > \text{Pb} > \text{Mn} > \text{Zn} > \text{Al}$. The HQ values for metals in both adults and children were found to be below 1.0, suggesting that these metals are present within acceptable level of non-carcinogenic health risk at all locations. Furthermore, we conducted an evaluation of the hazard index (HI) for each sample to gauge the overall potential non-carcinogenic effects of the examined heavy metals on human health. The HI values were calculated within the range of 1.26×10^{-1} to 1.59×10^{-1} , with an average of 1.36×10^{-1} for adults. For children, the HI values were 7.67×10^{-1} to 9.91×10^{-1} , with an average of 8.32×10^{-1} . Figure 6 displays the spatial distribution of the computed HI values, representing both adults

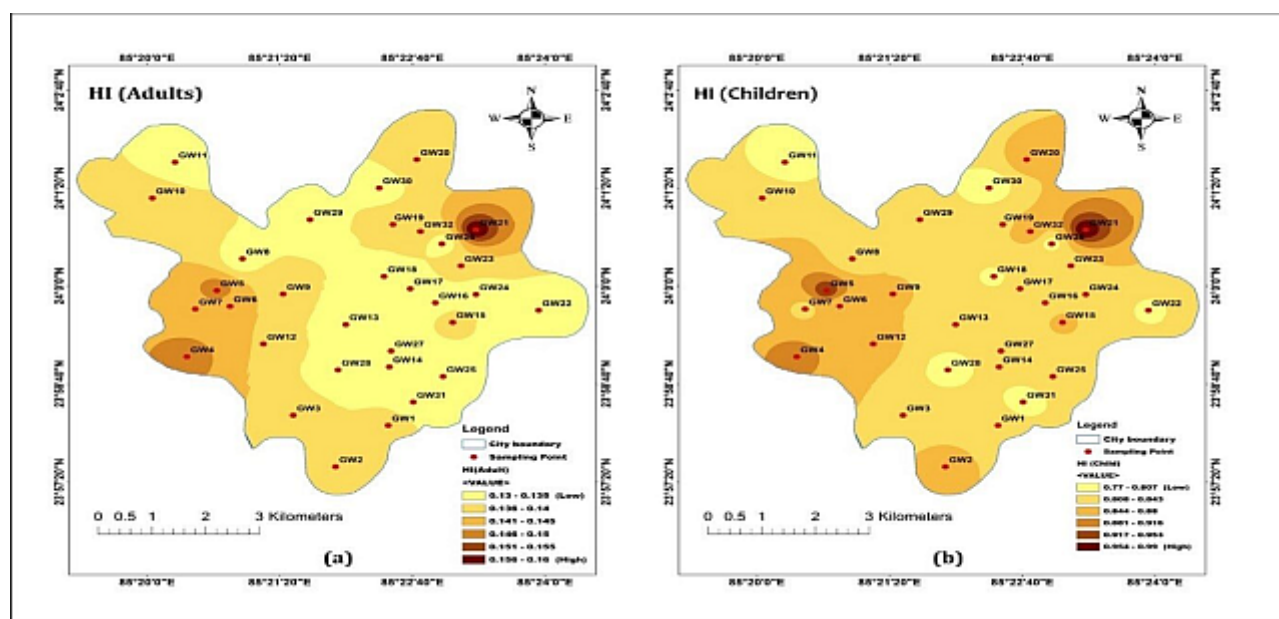


Figure 6. Spatial distribution map of (a) HI (Adults) and (b) HI (Children) of groundwater of study region

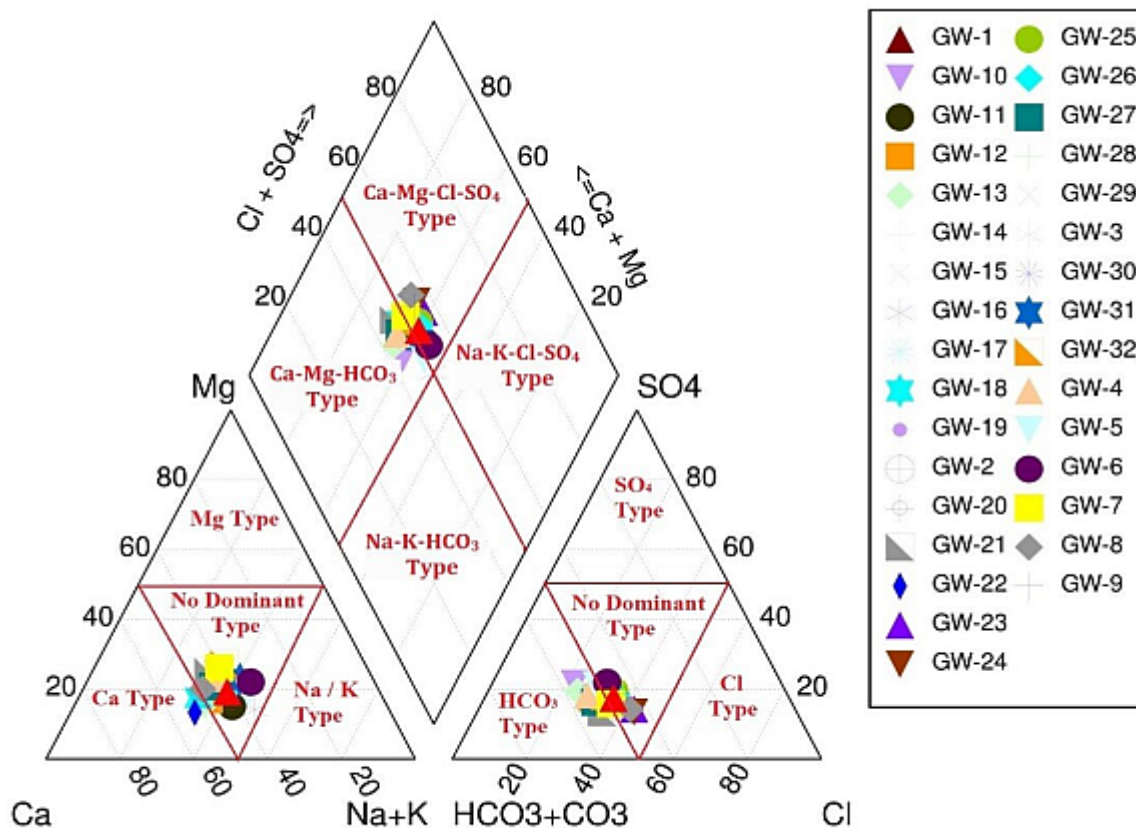


Figure 7. Piper trilinear diagram displaying hydrogeochemical facies of groundwater (Piper 1944)

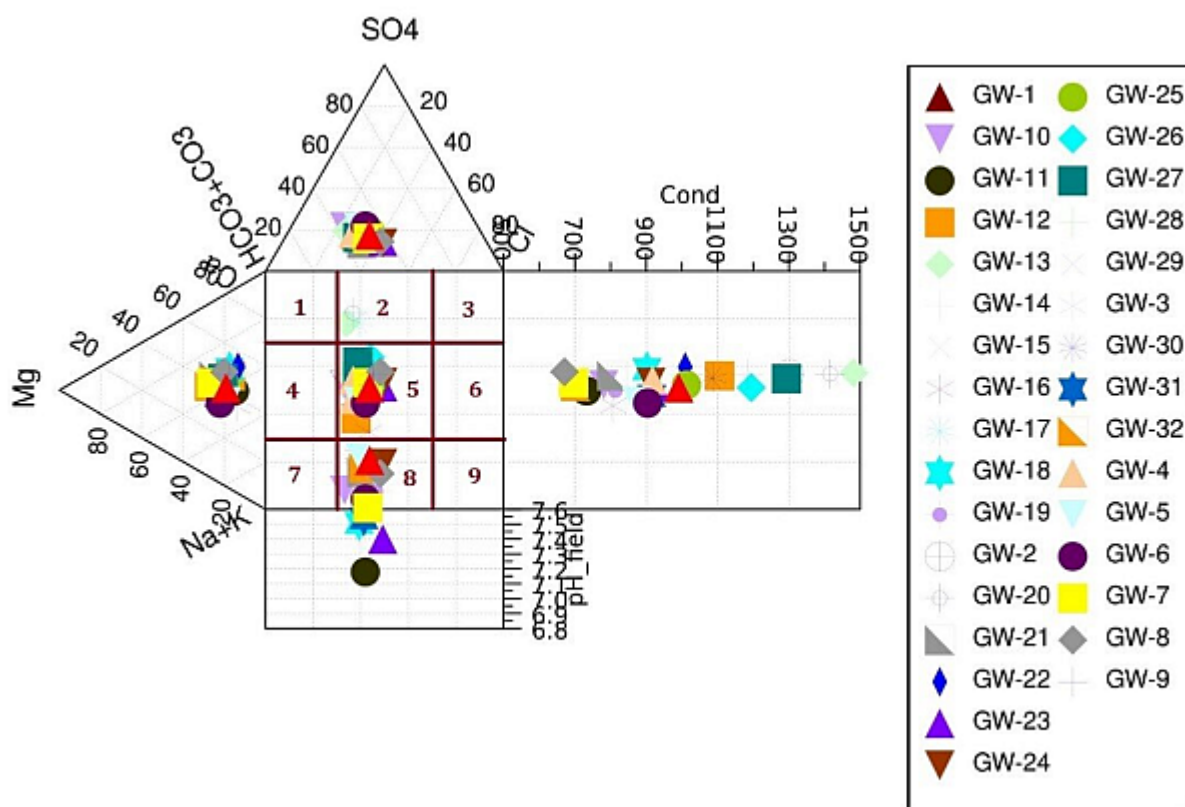


Figure 8. Durov diagram displaying hydrogeochemical facies of groundwater

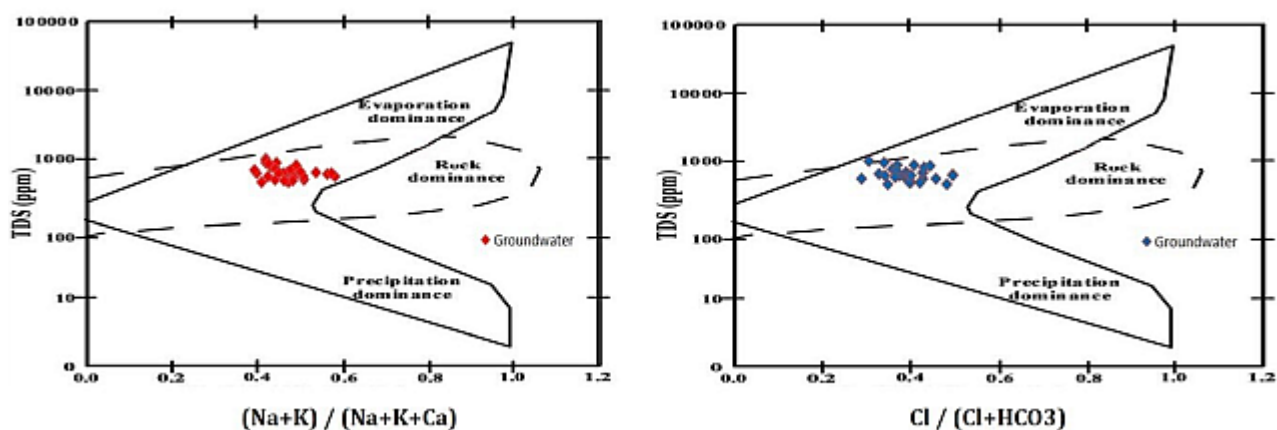


Figure 9. Gibbs diagram for Groundwater (GW) of the research area (Gibbs 1970)

and children, across various locations.

Hydro-geochemical analysis

Important details regarding the nature of groundwater are revealed by hydrogeochemical analysis, which depicts the chemical reaction that takes place when water permeates soil pores and rock cracks. The nature of the minerals that are in contact with water is revealed by several indices and plots.

The Piper diagram (Piper 1944), which classifies similar properties into categories, was used to identify commonalities in groundwater (Todd 1980). Accordingly, almost all groundwater samples show mixing types of cations except samples GW18 and GW22 which show Calcium-dominated water while 53% of groundwater is found to be Bicarbonate rich, and 47% of samples are of mixed type (Fig. 7). All the samples of groundwater belong to mixed regions of $\text{Ca}^{2+}\text{-Mg}^{2+}\text{-Cl-SO}_4^{2-}$ and $\text{Ca}^{2+}\text{-Mg}^{2+}\text{-HCO}_3^-$ type reflecting the prevalence of anthropogenic influence.

Tri-linear Durov Plot (Fig. 8) has been created using the recommended approach (Ravikumar et al. 2015, Young and Aston 1985), where the principal ion percentages are expressed in meq/L. According to the Durov plot, it is clear that 9.37% of groundwater samples exhibit association with dolomite or ion-exchange clay, 53.13% exhibit simple dissolution or mixing, and the rest 37.5 % reverse ion-exchange of Na-Cl type water.

The Gibbs diagram (Gibbs 1970) explains the relationship between the chemical elements present in water and indicates whether water samples fall under the dominance of precipitation, evaporation, or interaction of rock water. From the Gibbs diagram

(Fig. 9), it is obvious that all groundwater samples exhibit rock-water dominance.

Geochemical processes

The process that controls the chemistry of the groundwater in the study area is determined by the following geochemical processes that cause changes in groundwater quality and develop a strategy for groundwater protection.

Weathering and dissolution

When studying the solute contents in groundwater, the interactions between rocks and water, as well as evaporation, are important geochemical processes. These processes can be categorized into three main types: silicate weathering, carbonate dissolution, and evaporite dissolution (Tiwari and Singh 2014).

The bivariate plots depicted in Figure 10a,b illustrate the relationship between $\text{Ca}^{2+}/\text{Na}^+$ and $\text{HCO}_3^-/\text{Na}^+$ as well as $\text{Ca}^{2+}/\text{Na}^+$ and $\text{Mg}^{2+}/\text{Na}^+$. These plots provide evidence that silicate weathering is the predominant factor influencing these variables. The high content of HCO_3^- and a pH of less than 8.5 indicate occurrence of strong chemical weathering processes in the study area.

The interaction between $\text{Ca}^{2+} + \text{Mg}^{2+}$ and HCO_3^- in the study area is used to explain the mechanism of silicate weathering (Fig. 10c). The excess $\text{Ca}^{2+} + \text{Mg}^{2+}$ in all data points of surface water and groundwater above the 1:1 equiline suggests the necessity of alkalis to balance some of the carbonate alkalinity. Additionally, plot of $(\text{Na}^+ + \text{K}^+)$ versus total cations (Fig. 10d) further confirm the contribution of cations from silicate weathering (Elango et al. 2003, Rajmohan and Elango 2004). The higher ratio

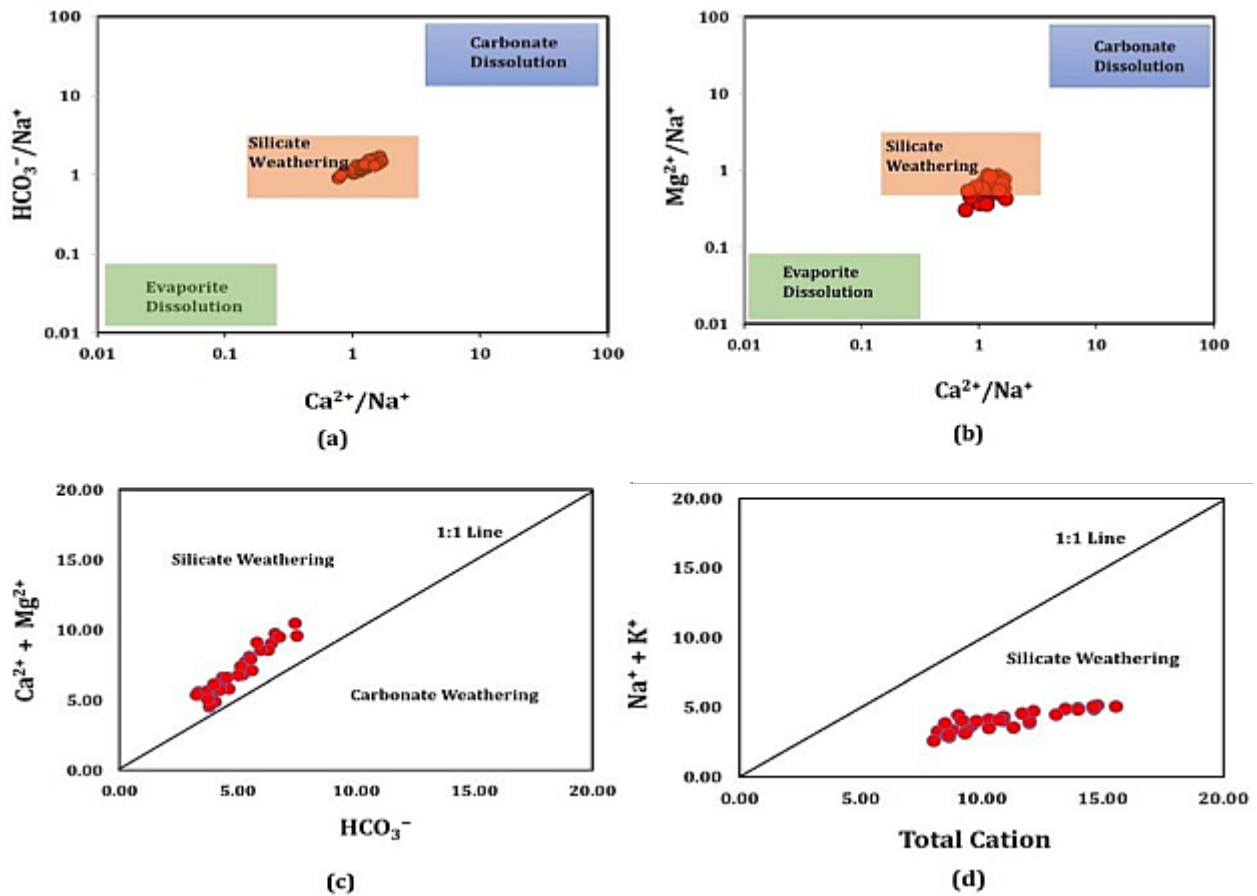


Figure 10. Bivariate Plots showing Silicate weathering as indicated by the relationships between (a) (Ca^{2+}/Na^+) vs. (HCO_3^-/Na^+) (b) (Ca^{2+}/Na^+) vs. (Mg^{2+}/Na^+) and (c) $(Ca^{2+} + Mg^{2+})$ vs. HCO_3^- (d) $(Na^+ + K^+)$ vs. total cations

of $(Na^+ + K^+) /$ total cation indicate that silicate weathering is the primary source of cation contribution. The study concludes that the weathering of silicates, including feldspars, calcic plagioclase, amphiboles, and pyroxenes, is the primary source of cations and HCO_3^- in the study area (Tiwari and Singh 2014).

Cation-exchange process

Cation exchange reactions play a significant role in controlling the origin and distribution of ions in groundwater. The identification of cation exchange processes can be done by studying the relationship between sodium and chloride ions. In a typical cation exchange process, sodium ions are added to water while calcium ions remain in the aquifer. Conversely, in the reverse cation exchange process, calcium ions are added to water while sodium ions remain in the aquifer (Elango et al. 2003). The calculation of Chloralkaline indices (CAI) I and II using equations xiv and xv also provides insights into the type of

cation exchange that dominates the groundwater. The results from Figure 11a,b suggest that reverse ion exchange prevails over normal cation exchange.

$$CAI I = Cl^- - \frac{Na^+_a + Cl^-}{Cl^-} \dots\dots\dots(xiv)$$

$$CAI II = Cl^- - \frac{Na^+_a + Cl^-}{SO_4^{2-} + HCO_3^- + CO_3^{2-} + NO_3^-} \dots\dots\dots(xv)$$

The concentration has been expressed in meq/L. Negative indices correspond to normal cation exchange, whereas positive indices indicate reverse ion exchange. In the research area, CAI I ranged from -0.189 to 3.485, while CAI II ranged from 1.298 to 4.006. These findings indicate the significant influence of cation exchange mechanisms on the groundwater chemistry in the investigated area.

Anthropogenic activity

The hydrochemistry of the study region is impacted by anthropogenic activities, including wastewater leakage from sewage tanks, which contribute to

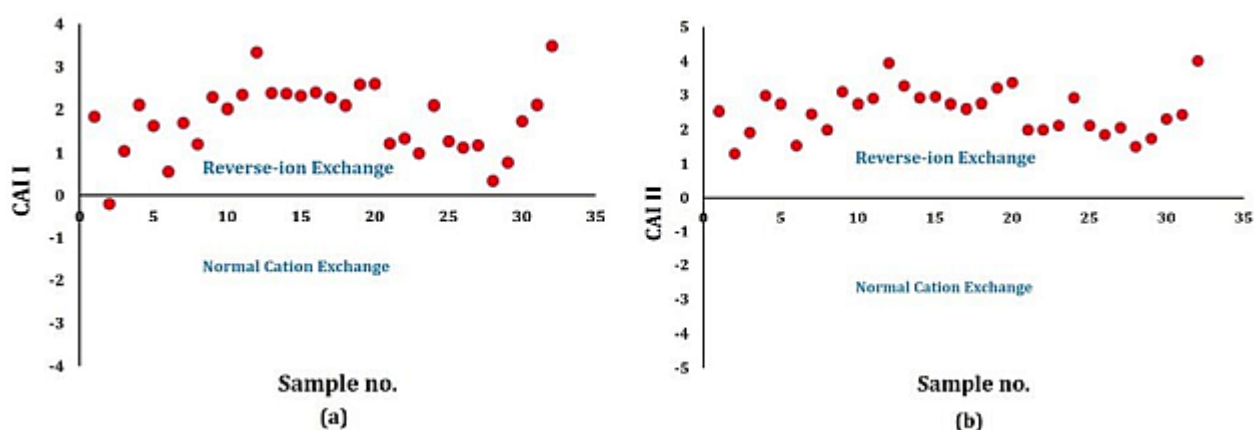


Figure 11. Plots showing reverse ion exchange (a) CAI I vs. Sample no. (b) CAI II vs. Sample no

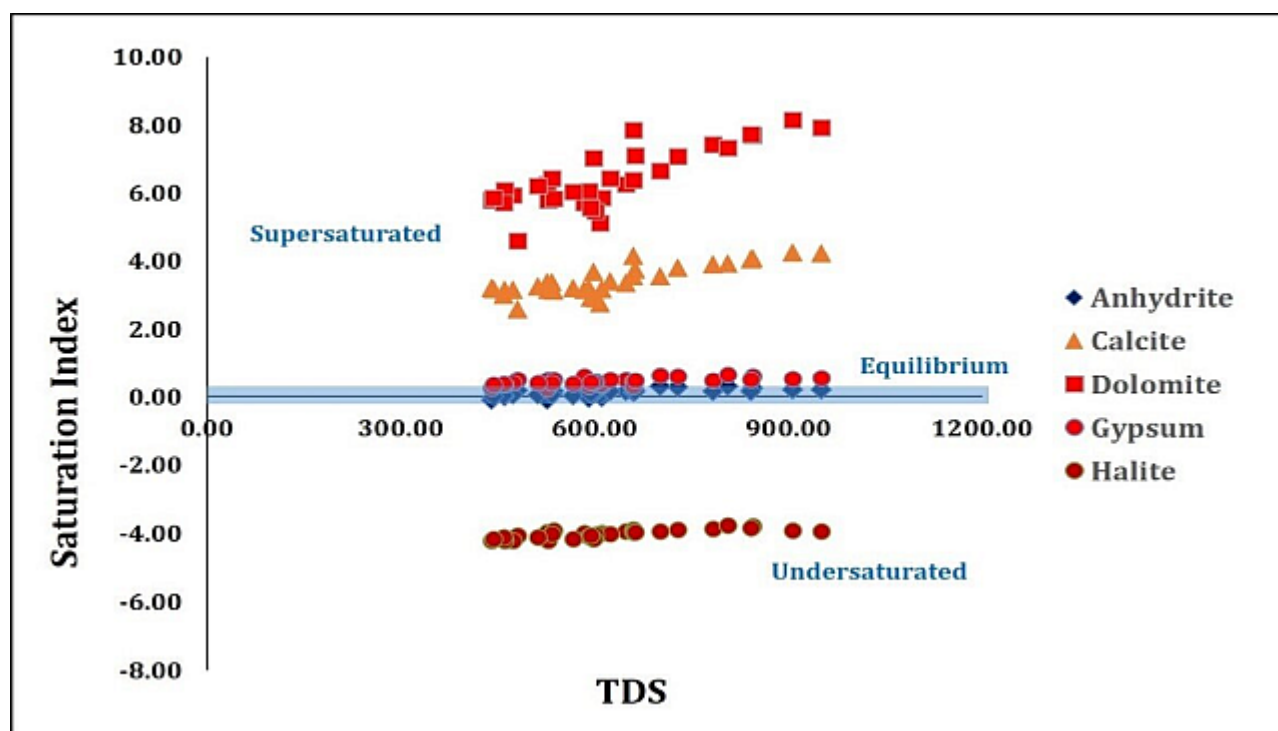


Figure 12. The plot of SI vs. TDS showing saturation indices of selected minerals

contamination (Sharma et. al. 2019). Observations made during field surveys revealed that the proximity of toilets, hand pumps, and tube wells in the area increases the likelihood of bacterial contamination in groundwater due to the absence of proper sanitary seals.

Saturation index

The saturation indices of various minerals including anhydrite, calcite, dolomite, gypsum, and halite were determined using PHREEQC software (Parkhurst and Appelo 1999). These saturation indices offer

important insights into the mineral composition of groundwater and the occurrence of precipitation and dissolution reactions (Appelo and Postma 2005). In the Hazaribag City region, groundwater was found to be oversaturated with calcite, dolomite and gypsum, indicating the possibility of their precipitation. The supersaturation of these minerals suggests that they are forming and may be present in sufficient quantities to reach equilibrium with the groundwater. While most of the samples are nearly equilibrium with anhydrite (Fig. 12), all 32

groundwater samples are undersaturated with halite, indicating their unsaturation and shorter residence time in the groundwater. The groundwater in the study area undergoes water-rock interactions during its flow from the runoff area to the discharge area. These interactions result in the groundwater reaching a state of equilibrium with minerals, causing an increase in total dissolved solids (TDS) as minerals dissolve progressively along the flow path.

Figure 12 depicting the saturation index versus TDS, offers valuable insights into the evolution of groundwater along the flow path. The saturation index values for calcite, dolomite and gypsum ranged from 2.58 to 4.24, 4.60 to 8.14 and 0.24 to 0.67, respectively (Table 5), but their correlations with TDS were not significant.

These findings indicate that the dissolution of these minerals does not persist along the flow path. Conversely, a significant portion of the samples (approximately 13%) exhibited saturation index values below zero for anhydrite and halite, showing

strong positive correlations with TDS (Fig. 12). This indicates that halite dissolves into groundwater along the flow path and increases TDS concentrations. The presence of anhydrite and halite leads to higher levels of Ca^{2+} and Na^+ in groundwater due to their dissolution.

Correlation coefficient of major cations and anions

A correlation matrix was utilized to investigate the interdependence among physiochemical variables in groundwater (Wu et al. 2014). The correlation coefficients were classified as low, good, and high, denoting values below 0.5, 0.5 and above 0.5, respectively. In this particular research area, a comprehensive collection and analysis of groundwater parameters were conducted, and the corresponding correlation matrix is provided in Table 6. It is evident from the correlation matrix that there is a strong association between EC and TDS. This can be attributed to the fact that higher TDS values increase the EC of water samples.

Additionally, HCO_3^- , SO_4^{2-} , Ca^{2+} , Mg^{2+} , Na^+ , and K^+ showed excellent correlations with EC, suggesting that they are the dominant ions in the area. The excellent correlation between HCO_3^- and SO_4^{2-} , as well as between HCO_3^- and Na^+ , is indicative of the weathering process. Moreover, positive correlations were found between HCO_3^- and Na^+ (0.78), HCO_3^- and Ca^{2+} (0.95), and HCO_3^- and K^+ (0.73), demonstrating that silicate materials react with water and carbon dioxide. The study also

Table 5. Summary of the mineral saturation index statistics in the study area

Saturation index	Minimum	Maximum	Mean	SD
SI Anhydrite	-0.10	0.32	0.12	0.11
SI Calcite	2.58	4.24	3.42	0.43
SI Dolomite	4.60	8.14	6.42	0.86
SI Gypsum	0.24	0.67	0.45	0.11
SI Halite	-4.23	-3.78	-4.02	0.12

Table 6. Correlation matrix of major cations and anions of the groundwater samples of the study region

Parameters	pH	Cond	TDS	Ca	Mg	Na	K	Cl	HCO_3	SO_4	F	NO_3
pH	1											
Cond	0.76**	1										
TDS	0.76**	1.00**	1									
Ca	0.67	0.82**	0.83	1								
Mg	0.53	0.62**	0.61	0.58	1							
Na	0.59	0.78**	0.78	0.71**	0.39	1						
K	0.71	0.88**	0.87	0.70	0.64	0.61	1					
Cl	0.54	0.69	0.71	0.74	0.57	0.56	0.59	1				
HCO_3	0.71**	0.85	0.85	0.95**	0.67	0.78**	0.73**	0.60	1			
SO_4	0.66	0.83**	0.83	0.80	0.62	0.79	0.74	0.56	0.84**	1		
F	0.66	0.50	0.50	0.55	0.44	0.58	0.48	0.48	0.59	0.51	1	
NO_3	0.24	0.17	0.16	0.17	0.01	0.09	0.15	0.15	0.12	0.11	0.13	1

** means correlation is significant

revealed a strong correlation between Na^+ and Ca^{2+} (0.71) and between HCO_3^- and pH (0.71) in the study region. The positive correlation of HCO_3^- and pH (0.71) suggests that pH is controlled by HCO_3^- .

Furthermore, the excellent correlation between Na^+ and Ca^{2+} (0.71) indicate that Na^+ in groundwater is replaced by Ca^{2+} in the aquifer during groundwater flow, resulting in low F^- concentration. Therefore, the cation exchange along groundwater flow and rock-water interaction contributes to the hydrogeochemical evolution of groundwater quality in the study region (Furi et al. 2011, 2012).

CONCLUSIONS

This research embodies hydrogeochemistry and water quality findings of Hazaribag City in the Hazaribag district of Jharkhand, India. On the basis of Schoeller diagram the major cations, anions, and heavy metals were found in the order $\text{Ca}^{2+} > \text{Na}^+ > \text{Mg}^{2+} > \text{K}^+$, $\text{HCO}_3^- > \text{Cl}^- > \text{SO}_4^{2-} > \text{NO}_3^-$, and $\text{Zn} > \text{Fe} > \text{Mn} > \text{Al} > \text{Cr} > \text{As} > \text{Pb}$, respectively. The hydrogeochemistry was studied with the help of different plots. The Gibbs Plot showed that rock-water interaction is the dominant mechanism in the area. The Piper plot demonstrated that groundwater samples are mixed regions of Ca^{2+} - Mg^{2+} - Cl^- - SO_4^{2-} and Ca^{2+} - Mg^{2+} - HCO_3^- type, reflecting the prevalence of anthropogenic influence. According to the Durov plot, 9.37% of groundwater samples exhibit association with dolomite or ion-exchange clay, 53.13% shows normal dissolution or mixing, and the rest 37.5 % reverse ion-exchange of sodium and chloride type water. The supersaturation of groundwater with respect to calcite, dolomite, and gypsum and the undersaturation with respect to halite, indicates that the groundwater is not in equilibrium and is still in an immature state.

The water quality index (WQI) indicated that only 9% of the groundwater samples were of good quality, 6% were poor, and 13% were very poor for human consumption. The rest of the samples, 72%, were unfit for drinking purposes. The high correlation between all water quality indices and heavy metals confirmed the contamination of the groundwater in Hazaribag City. The findings of the study suggest that the groundwater quality in Hazaribag City is poor and contaminated with heavy metals, making it

unsuitable drinking without treatment. The theoretical calculation of non-carcinogenic health risks assessment revealed that there are no potential health risks in the ground water.

The study's results have significant implications for the residents of Hazaribag City, who depend on groundwater for their daily needs. The findings highlight the need for immediate action to control mainly the TDS and pH of the groundwater to ensure safe drinking water sources for the community. In addition, the government and local authorities must take measures to prevent groundwater sources from mixing of pollutants due to anthropogenic activities. The study's results can also serve as a reference for similar studies in other regions facing similar challenges with water quality. Overall, the study emphasizes the importance of regular monitoring and assessment of water quality to ensure the provision of safe and clean water for communities.

ACKNOWLEDGEMENTS

The first author acknowledge the financial support from the UGC through senior research fellowship and Department of Chemistry, Vinoba Bhave University for the lab facilities. Help from the Retd. Prof. K.K. Srivastava who provided the required assistance in the statistical analysis is acknowledged.

Authors' contributions: Both the authors contributed equally

Conflict of interest: Authors declare no conflict of interest

REFERENCES

- Agrawal, V. and Jagetia, M. 1997. Hydrogeochemical assessment of groundwater quality in Udaipur city, Rajasthan, India. Pp. 151-154. In: Proceedings of National Conference on Dimension of Environmental Stress in India. Department of Geology, MS University, Baroda.
- Anonymous. 2006. Standard Methods for the Examination of Water and Waste. American Public Health Association, Washington DC.
- Anonymous. 2010. Human Health Risk Assessment: Risk-based Concentration Table. United States Environmental Protection Agency (USEPA), Washington DC.
- Anonymous. 2012. Indian standard specifications for drinking water. 10500: Bureau of Indian Standards, New Delhi, India.
- Anonymous. 2017. Monitoring health for the SDGs,

- Sustainable Development Goals, World Health Organization, Geneva.
- Appelo, C.A.J. and Postma, D. 2005. *Geochemistry, groundwater and pollution* (2nd ed.). A.A. Balkema Publishers, Leiden.
- Brown, R.M., McClelland, N.J., Deininger, R.A. and O'Connor, M.F. 1972. A Water Quality Index - Crossing the Psychological Barrier. Pp. 787-797. In: *Proceedings of the International Conference on Water Pollution Research*, Jerusalem.
- Chidambaram, S., Ramanathan, A.L., Anandhan, P., Srinivasamoorthy, K., Prasanna, M.V. and Vasudevan, S. 2008. A statistical approach to identify the hydro geochemically active regimes in ground waters of Erode district, Tamil Nadu. *Asian Journal of Water and Environmental Pollution*, 5(3), 123-135.
- Durvey, V.S., Sharma, L.L., Saini, V.P. and Sharma, B.K. 1991. *Handbook on the Methodology of Water Quality Assessment*. Rajasthan Agriculture University, India.
- Elango, L., Kannan, R. and Senthilkumar, M. 2003. Major ion chemistry and identification of processes of groundwater in the part of the Kancheepuram district, Tamilnadu, India, *Environmental Geoscience*, 10(4), 157-166. <https://doi.org/10.1306/eg100403011>.
- Foster, S., Chilton, J., Moench, M., Cardy, F. and Schifer, M. 2000. *Groundwater in rural development: facing the challenges of supply and resource sustainability*. World Bank Technical Paper 463. Washington, DC, USA.
- Furi, W., Razack, M., Abiye, T.A., Ayenew, T. and Legesse, D., 2011. Fluoride enrichment mechanism and geospatial distribution in the volcanic aquifers of the Middle Awash basin. *Northern Main Ethiopian Rift. Journal of African Earth Sciences*, 60, 315-327.
- Furi, W., Razack, M., Abiye, T.A., Kebede, S. and Legesse, D., 2012. Hydrochemical characterization of complex volcanic aquifers in a continental rifted zone: the Middle Awash basin, Ethiopia. *Hydrogeology Journal*, 20, 385-400. <https://doi.org/10.1007/s10040-011-0807-1>
- Garrels, R.M. 1976. A Survey of Low Temperature Water Mineral Relations. Pp. 65-84. In: *Interpretation of Environmental Isotope and Hydrogeochemical Data in Groundwater Hydrology*. International Atomic Energy Agency, Vienna.
- Gibbs, R.J. 1970. Mechanism controlling world water chemistry. *Science*, 170(3962), 1088-1090. [10.1126/science.170.3962.1088](https://doi.org/10.1126/science.170.3962.1088)
- Guettaf, M., Maoui, A. and Ihdene, Z. 2014. Assessment of water quality: A case study of the Seybouse River, North East of Algeria. *Applied Water Science*, 7, 295-307. <https://doi.org/10.1007/s13201-014-0245-z>.
- Gupta, S.K. and Gupta, I.C. 1987. *Management of Saline Soils and Water*. Oxford and IBH Publication Co., New Delhi. 399 pages.
- Hubbard, R.K. and Sheridan, J.M. 1989. Nitrate movement to groundwater in the southeastern coastal plain. *Journal of Soil Water Conservation*, 44, 20-27.
- Karanth, K.R. 1987. *Groundwater Assessment, Development and Management*. Tata-McGraw-Hill, New Delhi.
- Kaushik, A., Kumar, K. and Sharma, H.R. 2002. Water quality index and suitability assessment of urban groundwater of Hisar and Panipat in Haryana. *Journal of Environmental Biology*, 23, 325-333.
- Krishna Kumar, S., Bharani, R., Magesh, S., Prince and Chandrasekar, G.N. 2013. Hydrogeochemistry and groundwater quality appraisal of part of south Chennai coastal aquifers, Tamil Nadu, India using WQI and fuzzy logic method. *Applied Water Sciences*, 4, 341-350. <https://doi.org/10.1007/s13201-013-0148-4>.
- Kumar, A., Kumar, A. Lata, C., Kumar, S., Mangalassery, S., Singh, J.P., Mishra, A.K. and Dayal, D. 2018. Effect of salinity and alkalinity on responses of halophytic grasses *Sporobolus marginatus* and *Urochondra setulosa*. *Indian Journal of Agricultural Science*, 88 (8), 149-157.
- Means, B. 1989. *Risk-assessment Guidance for Superfund. Human Health Evaluation Manual. Part A. Interim Report (Final)*. Ofce of Solid Waste and Emergency Response, Environmental Protection Agency, Washington, DC (USA), 540, 1-89
- Meybeck, M. 1987. Global chemical weathering of surficial rocks estimated from river dissolved loads. *American Journal of Science*, 287, 401-428. <https://doi.org/10.2475/ajs.287.5.401>.
- Mohammadi, A.A., Zaei, A., Majidi, S., Ghaderpoury, A., Hashempour, Y., Saghi, M.H., Alinejad, A., Youse, M., Hosseingholizadeh, N. and Ghaderpoori, M. 2019. Carcinogenic and non-carcinogenic health risk assessment of heavy metals in drinking water of Khorramabad, Iran. *MethodsX*, 6, 1642-1651. <https://doi.org/10.1016/j.mex.2019.07.017>.
- Mohan, S.V., Nithila, P., and Reddy, S.J. 1996. Estimation of heavy metals in drinking water and development of heavy metal pollution index: *Journal Environmental Science Health Part A*, 31(2), 283-289. <https://doi.org/10.1080/10934529609376357>.
- Olayinka, A.I., Abimbola, A.F., Isibor, R.A., Rau, A.B. 1999. A geoelectric hydrochemical investigation of shallow groundwater occurrence in Ibadan, South Western Nigeria. *Environmental Geology*, 37, 31-39. <https://doi.org/10.1007/s002540050357>
- Parkhurst, D.L. and Appelo, C.A.J. 1999. *User's Guide to PHREEQC (Version 2) – A Computer Program for Speciation, Batch-Reaction, One-Dimensional Transport, and Inverse Geochemical Calculations*. U.S. Geological Survey Earth Science Information Center, Denver. <https://doi.org/10.3133/wri994259>.
- Piper, A.M. 1944. A graphic procedure in the geochemical interpretation of water analyses. *Eos, Transactions American Geophysical Union*, 25, 914-923. <https://doi.org/10.1029/TR025i006p00914>.
- Prince, M. 1985. *Introducing groundwater*, George Alien and Unwin, London, *Proceedings of an advisory group meeting*, IAEA, Vienna, 195 pages.
- Rajmohan, N. and Elango, L. 2004. Identification and evolution of hydrogeochemical processes in the groundwater environment in an area of the Palar and Cheyyar River Basins, Southern India. *Environmental Geology*, 46(1), 47-

61. <https://doi.org/10.1007/s00254-004-1012-5>.
- Ramesh, R. and Anbu, M. 1996. Chemical Methods for Environmental Analysis. Water and Sediment, Macmillan, London. 161 pages.
- Rao, B.K., Panchaksharjah, S., Patil, B.N., Narayana, A., Kaiker, D.L.S. 1982. Chemical composition of irrigation waters from selected parts of Bijpur district, Karnataka. Journal of Agricultural Science, 16(4), 426-432.
- Ravikumar, P., Somashekar, R. and Prakash, K.L. 2015. A comparative study on usage of Durov and Piper diagrams to interpret hydrochemical processes in groundwater from SRLIS river basin, Karnataka, India. Elixir Earth Science, 80, 31073-31077. <https://core.ac.uk/download/pdf/72804015.pdf>
- Schoeller, H. 1965. Qualitative evaluation of groundwater resources. Pp. 54–83. In: Methods and Techniques of Groundwater Investigations and Development, UNESCO, Paris,
- Sharma, S., Nagpal, A.K. and Kaur, I. 2019. Appraisal of heavy metal contents in groundwater and associated health hazards posed to human population of Ropar wetland, Punjab, India and its environs. Chemosphere, 227, 179-190. <https://doi.org/10.1016/j.chemosphere.2019.04.009>.
- Singh, R., Venkatesh, A.S., Syed, T.H., Reddy, A.G.S., Kumar, M. and Kurakalva, R.M. 2017. Assessment of potentially toxic trace elements contamination in groundwater resources of the coal mining area of the Korba coaled, Central India. Environmental Earth Sciences, 76, art566. <https://doi.org/10.1007/s12665-017-6899-8>.
- Tamasi, G. and Cini, R. 2004. Heavy metals in drinking waters from Mount Amiata (Tuscany, Italy): Possible risks from arsenic for public health in the Province of Siena. Science of Total Environment, 327, 41-51. <https://doi.org/10.1016/j.scitotenv.2003.10.011>.
- Tiwari, A.K. and Singh, A.K. 2014. Hydrogeochemical investigation and groundwater quality assessment of Pratapgarh district, Uttar Pradesh. Journal of Geological Society of India, 83(3), 329-343. <https://doi.org/10.1007/s12594-014-0045-y>.
- Todd, D.K. 1980. Groundwater Hydrology (2nd ed.). John Wiley and Sons, New York. 535 Pages.
- Wu, B., Zhao, D.Y., Jia, H.Y., Zhang, Y., Zhang, X.X., Cheng, S.P. 2009. Preliminary risk assessment of trace metal pollution in surface water from Yangtze River in Nanjing section, China. Bulletin of Environmental Contamination and Toxicology, 82, 405-409. <https://doi.org/10.1007/s00128-009-9673-0>.
- Wu, J.H., Li, P.Y., Qian, H. and Fang, Y. 2014. Assessment of soil salinization based on a low-cost method and its influencing factors in a semi-arid agricultural area, northwest China. Environmental Earth Sciences, 71, 3465-3475. <https://doi.org/10.1007/s12665-013-2736-x>.
- Young, D.A., Aston, T.R.C. 1985. Durov plot users guide: computer calculation and plotting of Durov diagrams for water chemistry analysis, Canada Center for Mineral and Energy Technology, Energy Research Program, Coal Research Laboratory, Report 85-78(TR), 13.

Received: 8th September 2023

Accepted: 20th December 2023